The Effect of Different Weighting Ratios, Length, and Thickness on Weighted Sum of the First Natural Frequency and Critical Buckling Load for a Laminated Composite Circular Cylindrical Shell

R. Ashrafian *, A. Ghoddosian

Department of Mechanical Engineering, Semnan University, P.O. Box 35131-19111, Semnan, Iran

ABSTRACT

In this study, a weighted sum, consisting two non-dimensionalized quantities critical buckling force and natural frequency, is employed to maximize the objective function for a laminated composite circular cylindrical shell. The function is considered to find the optimum solutions as the goal. Orientation angles of fibers are mentioned in a well-known configuration as candidate design, and critical buckling force and natural frequency values are derived with the first order shear deformation theory. The composite shell is considered with 8 layers, also the boundary conditions are assumed to be fully simply support and to satisfy boundary conditions displacement and slope components are defined in form of double Fourier series. After combination of differential operators and Fourier series, eventually the matrix L is found and Galerkin method gains function values. For this purpose, a program based on MATLAB is employed for the process. Validations of numerical results show that the used method is moderately satisfactory and acceptable in predicting the critical buckling force and the natural frequency of the shell in comparison with other works. As the conclusion, the effect of different weighting ratios, shell length-to-radius ratios, and shell thickness-to-radius ratios on the optimal designs are investigated and the results are compared.

1. Introduction

Composite physical properties are achieved by combining different materials to meet specific requirement. Enormous benefits that these materials posses attract researchers to explore more into it to script its behavior in a well-defined form to the users. On the other hand, the structures are quite often are subjected to in-plane or external loads which may cause buckling. In addition, the vibration can be problematic when the excitation frequency coincides with the shell's resonance frequency. Such loadings may occur at different times under in-service conditions, necessitating a design approach that is capable of taking in to account these various loading conditions.

In the recent years, numerical approaches are focused on the problems of the composite structures. For example, Liu et al. [1] investigated nonlinear breathing vibrations of an eccentric rotating composite laminated circular cylindrical shell, which is subjected to the lateral and temperature excitations. It was carried out based on Donnell thin shear deformation theory, von Kármán-type nonlinear relation and Hamilton's principle. Pitton et al. [2] by a methodology involving the design of an Artificial Neural Network (ANN) predicted the approximation of the buckling load and of the pre-buckling stiffness of a composites cylindrical shell. Zhang et al. [3] focused on the resonant responses and chaotic dynamics of a composite laminated circular cylindrical shell with radially pre-stretched membranes at both ends and clamped along a generatrix. Matsunaga [4] by employing the method of power series expansion of displacement components, a set of fundamental dynamic equations of a two-dimensional higherorder theory for laminated composite circular cylindrical shells made of elastic and orthotropic materials studied vibration and buckling through Hamilton's principle. Ungbhakorn, and Singhatanadgid [5] employed the similitude invariant and the scaling laws of the symmetric cross-ply laminated circular

* Corresponding author. Tel.: +989124606249
E-mail address: r.ashrafian@semnan.ac.ir

cylindrical shells for buckling and free vibration problems by applying the similitude transformation to the governing differential equations directly. Lam and Loy [6] studied the influence of boundary conditions for a thin laminated rotating cylindrical shell. The analysis was carried out using Love-type shell theory and solved using Galerkin's method. Lee [7] defined free vibration and dynamic response for the CFRP and GFRP cross-ply laminated circular cylindrical shells under impulse loads and investigated by using the first-order shear deformation shell theory. The modal analysis technique was used to develop the analytical solutions of the simply supported cylindrical shells. Walker and Smith [8] presented a methodology for using genetic algorithms with the finite element method to minimise a weighted sum of the mass and deflection of fibre reinforced structures with several design variables. Free vibration of laminated composite shells with cutouts are presented by a nine noded curved C0 finite element (FE) formulation developed by Kumar et al. [9] based on higher order shear deformation theory (HSDT) using Sander's approximations. A research by Sepiani et al. [10] investigated the free vibration and buckling of a two-layered cylindrical shell made of inner functionally graded (FG) and outer isotropic elastic layer, subjected to combined static and periodic axial forces. Wagner et al. [11] believed that the worst geometric imperfection is a mathematical concept which should deliver in theory a lower bound for the buckling load of unstiffened cylindrical shells, and the corresponding knock-down factors could be used as base for improved shell design guidelines in order to reduce weight and cost of unstiffened shells. The problem of local buckling of a thin composite laminated cylindrical shell under external pressure is studied by Mikhasev et al [12]. Geier et al. [13] by a research argued that the buckling loads of laminated cylinders can strongly depend on the position of the differently oriented layers within the shell. Labans et al. [14] presented a research that two laminated composite shells, one with a conventional straight fiber laminate denoted the classical laminated shell and the second one with a variable angle tow reinforced composite, had been excited and their natural frequencies and mode shapes had been measured and monitored as a function of the axial compression load. Ng and Lam [15] studied the vibration and critical speed of thin isotropic cylindrical shells under constant axial loads. In the analysis, Donnell's theory for a thin-walled cylindrical shell is used. Liu and chu [16] investigated Nonlinear vibrations of thin circular cylindrical shells. Based on Love thin shell theory, the governing partial differential equations of motion for the rotating circular cylindrical shell are formulated using Hamilton principle. Kassegne and chun [17] argued that Fiber reinforced composite materials continue to experience increased adoption in different employment. Walker et al. [18] obtained the multiobjective design of a symmetrically laminated shell with the objectives defined as the maximization of the axial and torsional buckling loads. The ply angle is taken as the optimizing variable.

Employing a weighted sum, consisting two non-dimensionalized quantities critical buckling force and natural frequency, is considered to maximize objective function for a laminated composite circular cylindrical shell. Orientation angles of fibers are considered as design variable. Critical buckling force and natural frequency values are derived with the first order shear deformation theory. Eventually, the effect of different weighting ratios, shell aspect ratio, and shell thickness-to-radius ratios on the optimal designs are investigated and the results are compared.

2. Governing Equations

A circular cylindrical shell, the schematic of the k-layer of the shell and coordinates are shown in Fig. 1. Based on first-order shear deformation theory, the equilibrium equations for a shell under axial loads N_a are as follows and the deformations are assumed to be small [19]:
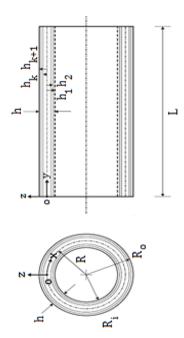

Fig. 1. K-layer laminated composite circular cylindrical shell and coordinate

$$\frac{\partial N_x}{\partial x} + \frac{\partial N_{x\varphi}}{R\partial \varphi} + q_x(x,\varphi,t)$$
$$= I_1 \frac{\partial^2 u}{\partial t^2} + I_2 \frac{\partial^2 \beta_x}{\partial t^2}$$

$$\frac{\partial N_{x\varphi}}{\partial x} + \frac{\partial N_\varphi}{R\partial \varphi} + \frac{Q_\varphi}{R} + N_a \frac{\partial^2 v}{\partial x^2}$$
$$+ q_\varphi(x,\varphi,t)$$
$$= \left(I_1 + \frac{2I_2}{R}\right)\frac{\partial^2 v}{\partial t^2}$$
$$+ \left(I_2 + \frac{I_3}{R}\right)\frac{\partial^2 \beta_\varphi}{\partial t^2}$$

$$\frac{\partial Q_x}{\partial x} + \frac{\partial Q_\varphi}{R\partial \varphi} - \frac{N_\varphi}{R} + N_a \frac{\partial^2 w}{\partial x^2} + q_r(x,\varphi,t)$$
$$= I_1 \frac{\partial^2 w}{\partial t^2}$$

$$\frac{\partial M_x}{\partial x} + \frac{\partial M_{x\varphi}}{R\partial \varphi} + m_x(x,\varphi,t) - Q_x$$
$$= I_2 \frac{\partial^2 u}{\partial t^2} + I_3 \frac{\partial^2 \beta_x}{\partial t^2}$$

$$\frac{\partial M_{x\varphi}}{\partial x} + \frac{\partial M_\varphi}{R\partial \varphi} + m_\varphi(x,\varphi,t) - Q_\varphi$$
$$= \left(I_2 + \frac{I_3}{R}\right)\frac{\partial^2 v}{\partial t^2}$$
$$+ I_3 \frac{\partial^2 \beta_\varphi}{\partial t^2}$$

(1)

I_1, I_2 and I_3 are defined by the following relation [19]:

$$(I_1, I_2, I_3) = \int_{\frac{-h}{2}}^{\frac{h}{2}} (1, z, z^2)\, \rho_k\, dz \tag{2}$$

All of the equivalent material properties for each layer is obtained with regard to 'rule of mixture'. Equation constitution of composite shell based on classical laminate theory are defined by the following relations [7]:

$$\begin{Bmatrix} N_x \\ N_\varphi \\ N_{x\varphi} \end{Bmatrix} = \begin{bmatrix} A_{11} & A_{12} & A_{16} \\ A_{12} & A_{22} & A_{26} \\ A_{16} & A_{26} & A_{66} \end{bmatrix} \begin{Bmatrix} \varepsilon_x^0 \\ \varepsilon_\varphi^0 \\ \gamma_{x\varphi}^0 \end{Bmatrix} + $$
$$\begin{bmatrix} B_{11} & B_{12} & B_{16} \\ B_{12} & B_{22} & B_{26} \\ B_{16} & B_{26} & B_{66} \end{bmatrix} \begin{Bmatrix} \kappa_x^0 \\ \kappa_\varphi^0 \\ \kappa_{x\varphi}^0 \end{Bmatrix}$$

$$\begin{Bmatrix} M_x \\ M_\varphi \\ M_{x\varphi} \end{Bmatrix} = \begin{bmatrix} B_{11} & B_{12} & B_{16} \\ B_{12} & B_{22} & B_{26} \\ B_{16} & B_{26} & B_{66} \end{bmatrix} \begin{Bmatrix} \varepsilon_x^0 \\ \varepsilon_\varphi^0 \\ \gamma_{x\varphi}^0 \end{Bmatrix} + $$
$$\begin{bmatrix} D_{11} & D_{12} & D_{16} \\ D_{12} & D_{22} & D_{26} \\ D_{16} & D_{26} & D_{66} \end{bmatrix} \begin{Bmatrix} \kappa_x^0 \\ \kappa_\varphi^0 \\ \kappa_{x\varphi}^0 \end{Bmatrix}$$

(3)

$$\begin{Bmatrix} Q_x \\ Q_\varphi \end{Bmatrix} = \begin{bmatrix} H_{55} & H_{45} \\ H_{45} & H_{44} \end{bmatrix} \begin{Bmatrix} \gamma_{xz}^0 \\ \gamma_{\varphi z}^0 \end{Bmatrix}$$

The *A*, *B*, *D*, and *H* matrices are defined as follows, where [19]:

$$A_{ij} = \sum_{k=1}^N (\bar{Q}_{ij})_k (h_k - h_{k-1})$$

$$B_{ij} = \frac{1}{2}\sum_{k=1}^N (\bar{Q}_{ij})_k (h_k{}^2 - h_{k-1}{}^2)$$

$$D_{ij} = \frac{1}{3}\sum_{k=1}^N (\bar{Q}_{ij})_k (h_k{}^3 - h_{k-1}{}^3)$$

$$H_{ij} = k_0 \sum_{k=1}^N (\bar{Q}_{ij})_k (h_k - h_{k-1})$$

(4)

$$\begin{Bmatrix} \varepsilon_x^0 \\ \varepsilon_\varphi^0 \\ \gamma_{x\varphi}^0 \end{Bmatrix} = \begin{Bmatrix} \dfrac{\partial u}{\partial x} \\ \dfrac{\partial v}{R\partial \varphi} + \dfrac{w}{R} \\ \dfrac{\partial u}{R\partial \varphi} + \dfrac{\partial v}{\partial x} \end{Bmatrix}$$

(5)

$$\begin{Bmatrix} \kappa_x^0 \\ \kappa_\varphi^0 \\ \kappa_{x\varphi}^0 \end{Bmatrix} = \begin{Bmatrix} \dfrac{\partial \beta_x}{\partial x} \\ \dfrac{\partial \beta_\varphi}{R\partial \varphi} \\ \dfrac{\partial \beta_x}{R\partial \varphi} + \dfrac{\partial \beta_\varphi}{\partial x} \end{Bmatrix}$$

$$\begin{Bmatrix} \gamma_{xz}^0 \\ \gamma_{\varphi z}^0 \end{Bmatrix} = \begin{Bmatrix} \beta_x + \dfrac{\partial w}{\partial x} \\ \beta_\varphi + \dfrac{\partial w}{R\partial \varphi} - \dfrac{v}{R} \end{Bmatrix}$$

k_0 equals $\frac{\pi^2}{12}$ in the last portion of Eq. (4). Then [19]:

$$\bar{Q}_{11} = Q_{11} \cos^4\theta + 2(Q_{12} + 2Q_{66})\sin^2\theta \cos^2\theta + Q_{22}\sin^4\theta$$

$$\bar{Q}_{12} = (Q_{11} + Q_{22} - 4Q_{66})\sin^2\theta \cos^2\theta + Q_{12}(\sin^4\theta + \cos^4\theta)$$

$$\bar{Q}_{22} = Q_{11}\sin^4\theta + 2(Q_{12} + 2Q_{66})\sin^2\theta \cos^2\theta + Q_{22}\cos^4\theta$$

$$\bar{Q}_{16} = (Q_{11} - Q_{12} - 2Q_{66})\sin\theta \cos^3\theta + (Q_{12} - Q_{22} + 2Q_{66})\cos\theta \sin^3\theta$$

$$\bar{Q}_{26} = (Q_{11} - Q_{12} - 2Q_{66})\cos\theta \sin^3\theta + (Q_{12} - Q_{22} + 2Q_{66})\sin\theta \cos^3\theta$$

(6)

$$\bar{Q}_{66} = (Q_{11} + Q_{22} - 2Q_{12} - 2Q_{66})\sin^2\theta \cos^2\theta + Q_{66}(\sin^4\theta + \cos^4\theta)$$

$$\bar{Q}_{44} = Q_{44}\cos^2\theta + Q_{55}\sin^2\theta$$

$$\bar{Q}_{45} = (Q_{55} - Q_{44})\sin\theta \cos\theta$$

$$\bar{Q}_{55} = Q_{55}\cos^2\theta + Q_{44}\sin^2\theta$$

$$Q_{11} = \frac{E_1}{1 - \nu_{12}\nu_{21}}$$

$$Q_{12} = \frac{\nu_{12}E_2}{1 - \nu_{12}\nu_{21}}$$

$$Q_{22} = \frac{E_2}{1 - \nu_{12}\nu_{21}}$$

$$Q_{66} = G_{12} \quad Q_{44} = G_{23} \quad Q_{55} = G_{13}$$

3. Boundary Conditions

The boundary conditions for the cylindrical shell with fully simply support are considered as [10]:

$$N_x(0,\varphi,t) = N_x(L,\varphi,t) = 0$$

$$M_x(0,\varphi,t) = M_x(L,\varphi,t) = 0$$

$$w(0,\varphi,t) = w(L,\varphi,t) = 0 \tag{7}$$

$$v(0,\varphi,t) = v(L,\varphi,t) = 0$$

The external excitations are taken to be zero in order to solve the buckling and free vibration problems. After substituting Eq. (7) into the equations of motion, the results are simplified in the following form:

$$[L]\{U\} = \{0\} \tag{8}$$

where:

$$L = \begin{bmatrix} L_{11} & L_{12} & L_{13} & L_{14} & L_{15} \\ L_{21} & L_{22} & L_{23} & L_{24} & L_{25} \\ L_{31} & L_{32} & L_{33} & L_{34} & L_{35} \\ L_{41} & L_{42} & L_{43} & L_{44} & L_{45} \\ L_{51} & L_{52} & L_{53} & L_{54} & L_{55} \end{bmatrix}$$

$$\{U\} = \begin{Bmatrix} u(x,\varphi,t) \\ v(x,\varphi,t) \\ w(x,\varphi,t) \\ \beta_x(x,\varphi,t) \\ \beta_\varphi(x,\varphi,t) \end{Bmatrix} \tag{9}$$

All components of matrix L are expanded in the appendix segment. To satisfy the boundary conditions, u, v, w, β_x and β_φ are defined by the following double Fourier series [7]:

$$u = \sum_m \sum_n \bar{A}_{mn} T_{mn}(t)$$
$$= \sum_m \sum_n A_{mn} \cos\left(\frac{m\pi x}{L}\right) \cos(n\varphi) T_{mn}(t)$$

$$v = \sum_m \sum_n \bar{B}_{mn} T_{mn}(t)$$
$$= \sum_m \sum_n B_{mn} \sin\left(\frac{m\pi x}{L}\right) \sin(n\varphi) T_{mn}(t) \tag{10}$$

$$w = \sum_m \sum_n \bar{C}_{mn} T_{mn}(t)$$
$$= \sum_m \sum_n C_{mn} \sin\left(\frac{m\pi x}{L}\right) \cos(n\varphi) T_{mn}(t)$$

$$\beta_x = \sum_m \sum_n \bar{D}_{mn} T_{mn}(t)$$
$$= \sum_m \sum_n D_{mn} \cos\left(\frac{m\pi x}{L}\right) \cos(n\varphi) T_{mn}(t)$$

$$\beta_\varphi = \sum_m \sum_n \bar{E}_{mn} T_{mn}(t)$$
$$= \sum_m \sum_n E_{mn} \sin\left(\frac{m\pi x}{L}\right) \sin(n\varphi) T_{mn}(t)$$

T is the function of time in the above equations. Also A, B, C, D and E are the constant coefficients of the natural mode shapes. Galerkin method is employed to solve the differential equations [6].

$$\int_0^t \int_0^{2\pi} \int_0^L (L_{11}u + L_{12}v + L_{13}w + L_{14}\beta_x + L_{15}\beta_\varphi) \cos(n\varphi) dx d\varphi dt = 0$$

$$\int_0^t \int_0^{2\pi} \int_0^L (L_{21}u + L_{22}v + L_{23}w + L_{24}\beta_x + L_{25}\beta_\varphi) \sin(n\varphi) dx d\varphi dt = 0$$

$$\int_0^t \int_0^{2\pi} \int_0^L (L_{31}u + L_{32}v + L_{33}w + L_{34}\beta_x + L_{35}\beta_\varphi) \cos(n\varphi) dx d\varphi dt = 0 \tag{11}$$

$$\int_0^t \int_0^{2\pi} \int_0^L (L_{41}u + L_{42}v + L_{43}w + L_{44}\beta_x + L_{45}\beta_\varphi) \cos(n\varphi) dx d\varphi dt = 0$$

$$\int_0^t \int_0^{2\pi} \int_0^L (L_{51}u + L_{52}v + L_{53}w + L_{54}\beta_x + L_{55}\beta_\varphi) \sin(n\varphi) dx d\varphi dt = 0$$

4. Buckling Analysis

In the buckling analysis, the material and the geometry of the shell are assumed to be perfect and no imperfection exists. To calculate the buckling load, the static solution is performed (i.e. $T = 0$). After Solving Eq. (8) by Galerkin method and its simplification, the following equation was obtained [5]:

$$[C_{ij}]\{A_{mn} \ B_{mn} \ C_{mn} \ D_{mn} \ E_{mn}\}^T = 0 \ (i,j = 1,...,5) \tag{12}$$

Determinant of the coefficients C_{ij} is set to be zero; thus, the buckling loads equation is derived as [5]:

$$\gamma_1 N_{cr}^2 + \gamma_2 N_{cr} + \gamma_3 = 0 \tag{13}$$

In Eq. (13), γ_i are the constant coefficients and N_{cr} is the axial critical buckling load [5].

5. Free Vibration Analysis

To solve the free vibration problem, the function of time is assumed as follows [5]:

$$T_{mn}(t) = e^{-i\omega_{mn}t} \tag{14}$$

A method similar to the buckling analysis method is employed to be derived the following set of equations [5]:

$$\left[[K_{ij}] - \omega_{mn}^2 [M_{ij}] \right] \{ A_{mn} \ B_{mn} \ C_{mn} \ D_{mn} \ E_{mn} \}^T = 0 \tag{15}$$

$$(i, j = 1, \dots, 5)$$

The determinant of the coefficients is set to be zero, thus the characteristic frequency equation is derived as [5]:

$$\delta_1 \omega^{10} + \delta_2 \omega^8 + \delta_3 \omega^6 + \delta_4 \omega^4 + \delta_5 \omega^2 + \delta_6 \omega = 0 \tag{16}$$

where δ_i are the constant coefficients, after solving the Eq. (16), natural frequencies are calculated, and substitution of these frequencies in Eq. (15) infer the constant coefficients of the mode shapes [5].

6. Problem Formulation

The following non-dimensionalized quantities are introduced to the all computations [8]:

$$N^* = \frac{N_{cr}}{N_0} \quad F^* = \frac{f_{cr}}{f_0} \tag{17}$$

where N_0 and f_0 correspond to lamination angles $(0°, 0°, 0°, 0°)_{sym}$ for eight layers. Maximization of the fundamental natural frequency and critical buckling load of the shell with the laminate configurations given by a combination of $\theta, 0°, 90°$ ply angles is considered as a optimization problem to find the best orientation angles of fibres in the laminated cylindrical shells. The objective function, OF, can be describes as follows [8]:

$$OF = \alpha F^* + \beta N^* \tag{18}$$

where α and β are the weighting factors which have following conditions $\alpha, \beta \geq 0, \alpha + \beta = 1$. As the first case, the single objective designs can be obtained as special cases by setting $\alpha=0$ or $\alpha =1$. As the second case, to equalize the effect of each component of the objective function formula (OF), α should be set to 0.5. Furthermore, $\alpha=0.25$ or $\alpha=0.75$ provide a space between the first case

and the second case. In this study, five laminate configurations are considered as candidate designs [8].

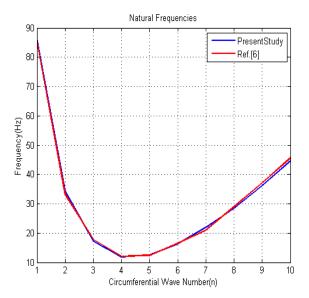## 7. Verification and Numerical Result

The material properties related to Fig. 2 are shown in Table 2. Fig. 2 indicates the comparison between the frequency results for a fully simply supported (SSSS) boundary condition of the shell for the present research and Ref. [6]. To ensure the accuracy of the model for buckling of the cylindrical shell, the buckling loads obtained by Ref. [5] was compared with the same results obtained by the present work. Table 4 shows the discrepancy between the results. Table 3, shows the ply properties of the composites used in Table 4 and Ref. [5]. As it is shown in Figs. 2 and Table 4, the results are in good agreement.

The numbers (m, n) in the parenthesis represent the buckling modes, i.e., number of axial half waves (m) and number of circumferential waves (n).

Numerical results are given for graphite/epoxy material, and the laminated cylindrical shell is constructed of equal thickness layers. *H/R = 0.2* and *L/R = 1* are considered.

Table 1. Laminate Configurations

Prompt	Laminate Configuration
C1	$(\theta°, -\theta°, \theta°, -\theta°)_{sym}$
C2	$(\theta°, -\theta°, 90°, 0°)_{sym}$
C3	$(\theta°, -\theta°, 0°, 0°)_{sym}$
C4	$(\theta°, \theta°, 0°, 90°)_{sym}$
C5	$(\theta°, \theta°, 90°, 90°)_{sym}$

Fig. 2 Comparison of variation of frequency with circumferential wave number for the SSSS composite cylindrical shell with Ref. [6], $h/R = 0.002$, $L/R = 20$, stacking sequence: [90/0/90]

Table 2. Relative material properties with Fig. 2

E_{11} (GPa)	E_{22} (GPa)	G_{12} (GPa)	G_{13} (GPa)	G_{23} (GPa)	ν_{12}	ρ $\left(\dfrac{\text{kg}}{\text{m}^3}\right)$
19	7.6	4.1	4.1	4.1	0.26	1643

Table 3. Ply properties of the composites used in Ref. [5]

	Ply Thickness (mm)	ν_{12}	G_{12} (GPa)	E_{22} (GPa)	E_{11} (GPa)
Graphite/Epoxy	0.127	0.24	5.65	10.8	132
Kevlar/Epoxy	0.127	0.34	2.07	5.50	76.8
E-glass/Epoxy	0.127	0.26	4.14	8.27	38.6

Table 4. Comparison between the results for buckling loads of a simply supported anisotropic cross-ply cylindrical shell with the lay up $[0/90]_{2s}$, $R = 0.2$

Configuration		Buckling Loads (KN/m)		
Material	Ratio (L/R)	Present Study	Ref. [5]	Discripancy (%)
Graphite/Epoxy	1	85.44 (11,3)	84.23 (11,3)	1.41
	3	85.44 (11,9)	84.23 (11,9)	1.41
Kevlar/Epoxy	1	41.09 (10,3)	39.38 (10,3)	4.16
	2	40.62 (10,5)	38.96 (10,5)	4.08
E-glass/Epoxy	1	43.72 (12,3)	42.97 (12,3)	1.71
	3	43.72 (12,9)	42.97 (12,9)	1.71

7.1. Effect of weighting ratios on the results

The effect of five different weighting ratios on the optimal results is given for different five laminate configurations in Figs. 3 and 4 and Table 5. As seen from Fig. 3 and 4, the best laminate configuration is *C1* for all the quantities of α. The *(OF)$_{MAX}$* is almost the same for *C2*, *C3*, *C4*, and *C5* laminate configurations, whereas *C1* is completely different, and obtain the best quantity of *OF* 1.97 with Theta(θ) 39.43. As seen from Fig. 3 and 4, as the weighting ratio increases, the *(OF)$_{MAX}$* decreases for all the states. Overall *C1* displays the best result and maximized *OF* amongst other states. The best fiber angle in Fig. 3 varies around 40. As mentioned above, the largest amount assigned to the objective function was 1.97. This value belonged to α=0. This truely indicate the greater importance and influence of natural frequency than critical buckling force. Therefore, the values and orientasion angles of fiber that lead to the maximum values of the natural frequency will most definitely have the maximum values of the weight function.

7.2. Effect of shell lengths on the results

The effect of shell lengths on the optimal results is given in Fig. 5 for five laminate configurations. As seen from the figure, as the shell length increases, the *OF* decreases. Also, the best fiber angle decreases for all state's despite of the rise of shell lengths, with the exception of *C1*. The optimum fiber angles and *(OF)$_{max}$* are given for all laminate configurations for shell lengths in Table 6.

7.3. Effect of shell thickness on the results

The effect of shell thickness on the optimal results is given in Fig. 7 for five different laminate configurations. As seen from Fig. 7, as the shell thickness increases, the OF increases. Each case of the Fig. 7 clearly demonstrate an intersection between 70 deg and 80 deg. The best fiber orientation angles for all cases alters in 40 deg approximately. The optimum fiber angles and *(OF)$_{max}$* are given for all laminate configurations for shell thickness in Table 7.
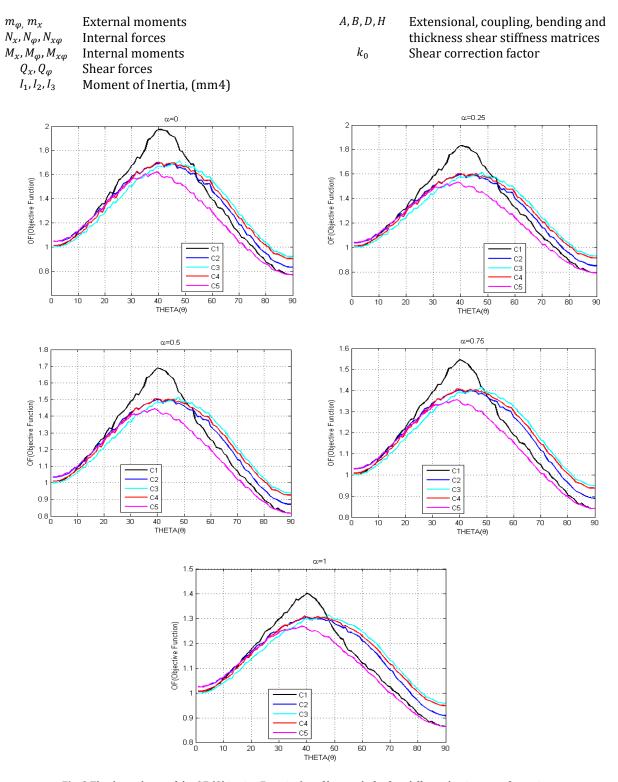
8. Conclusions

In this study, maximization of a weighted sum of the frequency and buckling load under external load for laminated composite circular cylindrical shell is investigated. Five shell configurations with eight layers are considered as candidate designs. The best design enjoys the highest quantity for *OF*, which equals to a weighted sum of the objectives non-dimensionalized quantities of the critical buckling force and the first natural frequency.

Present results can lead designer to apply optimal laminate configuration which can be functional in an acceptable manner. The effect of different weighting ratios, length, and thickness on the optimal results are investigated. Graphs, demonstrating the relation of the fiber angle with *OF*, illustrate that the maximum *OF* occurs at a specific value of the fiber angle and this value can be several times higher than the *OF* at other fiber angles. This fact emphasizes the importance of optimization in modern design to obtain the best performance of laminated composite shells. Eventually, it can be said that the fundamental frequency generally has a more significant effect than the buckling load on the maximum *OF*, and the weighting ratio generally has not a marked effect on the fiber angles.

Nomenclature

R	Radius, (mm)
L	Length, (mm)
H	Thickness, (mm)
u, v, w	Displacement components in the axial, tangential and radial directions
q_x, q_φ, q_r	External forces

m_φ, m_x	External moments	A, B, D, H	Extensional, coupling, bending and
$N_x, N_\varphi, N_{x\varphi}$	Internal forces		thickness shear stiffness matrices
$M_x, M_\varphi, M_{x\varphi}$	Internal moments	k_0	Shear correction factor
Q_x, Q_φ	Shear forces		
I_1, I_2, I_3	Moment of Inertia, (mm4)		

Fig. 3 The dependence of the OF (Objective Function) on fibre angle for five different laminate configurations

Table. 5 The best configurations and (Objective Function) MAX of the five different candidates for weighting ratios

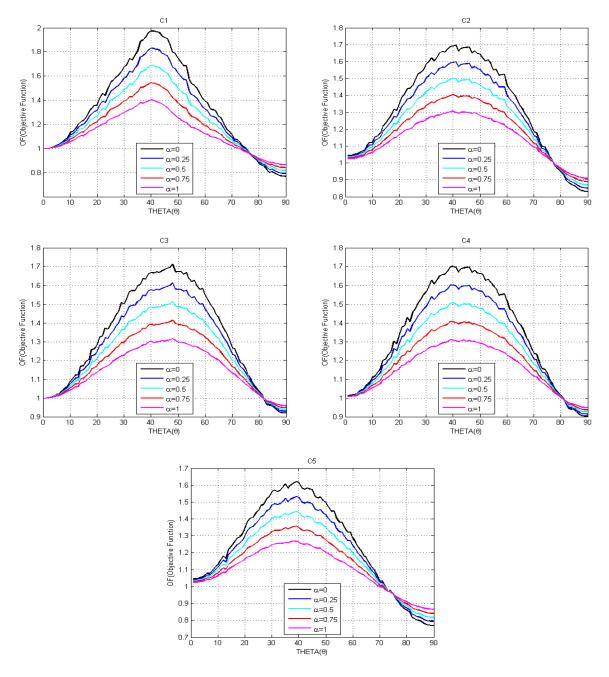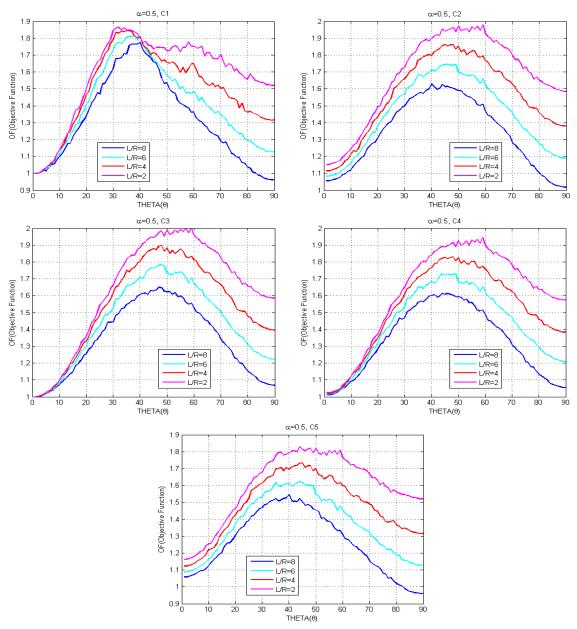| Laminate Configuratio	$\theta_{opt}(°)$						$(OF)_{MAX}$				
	$\alpha = 0$	$\alpha = 0.25$	$\alpha = 0.5$	$\alpha = 0.75$	$\alpha = 1$		$\alpha = 0$	$\alpha = 0.25$	$\alpha = 0.5$	$\alpha = 0.75$	$\alpha = 1$
C1	39.43	39.43	39.43	39.43	39.43		1.97	1.83	1.68	1.54	1.40
C2	40.44	40.44	39.43	39.43	39.43		1.69	1.59	1.49	1.40	1.30
C3	47.52	47.52	47.52	47.52	47.52		1.71	1.61	1.51	1.41	1.31
C4	39.43	39.43	38.42	38.42	38.42		1.70	1.60	1.50	1.40	1.31
C5	38.42	38.42	38.42	38.42	37.41		1.61	1.53	1.44	1.35	1.26

Fig. 4 The dependence of the OF (Objective Function) on fibre angle for different weighting ratios

Table. 6 The best configurations and (Objective Function) $_{MAX}$ of the five different candidates for *L/R* ratio

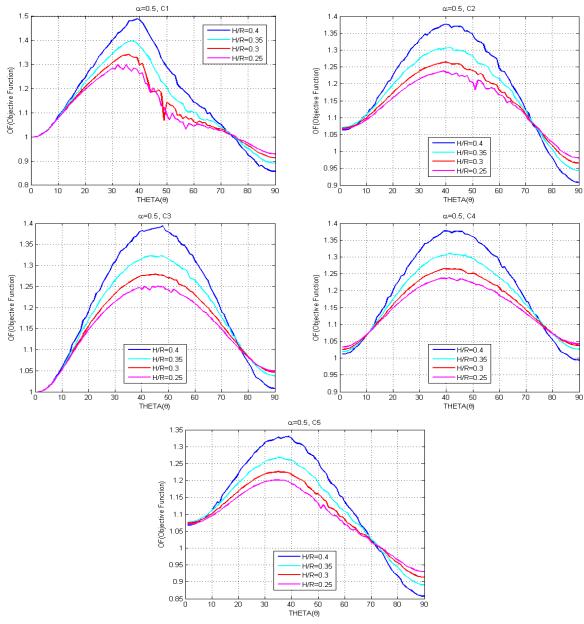| Laminate	$\theta_{opt}(°)$				$(OF)_{MAX}$			
Configuration	$L/R = 2$	$L/R = 4$	$L/R = 6$	$L/R = 8$	$L/R = 2$	$L/R = 4$	$L/R = 6$	$L/R = 8$
C1	32.06	34.25	37.04	40.08	1.86	1.84	1.81	1.77
C2	59.02	46.2	45.81	40.04	1.98	1.86	1.74	1.63
C3	59.51	48.14	47.71	47.54	1.99	1.89	1.78	1.64
C4	59.78	47.31	48.62	45.05	1.94	1.83	1.73	1.61
C5	44.23	44.54	43.89	40.14	1.83	1.73	1.62	1.54

Fig. 5 Effect of shell length on the optimal results for different five laminate configurations ($H/R = 0.2$, $\alpha = 0.5$).

Table. 7 The best configurations and (Objective Function) $_{MAX}$ of the five different candidates for H/R ratio

Laminate Confirnation	$\theta_{opt}(°)$				$(OF)_{MAX}$			
	$H/R = 0.4$	$H/R = 0.35$	$H/R = 0.30$	$H/R = 0.25$	$H/R = 0.4$	$H/R = 0.35$	$H/R = 0.30$	$H/R = 0.25$
C1	39.52	38.17	36.24	32.26	1.48	1.39	1.34	1.30
C2	40	41.48	40.04	38.2	1.37	1.30	1.26	1.23
C3	47.54	44.48	45.14	41.58	1.39	1.32	1.27	1.25
C4	40.09	42.29	41.48	41.28	1.37	1.31	1.26	1.23
C5	39.43	35.61	35.23	34.16	1.32	1.26	1.22	1.20

$\bar{Q}$	Transformed stiffness matrix	$\varepsilon_x^0, \varepsilon_\varphi^0, \gamma_{x\varphi}^0$	Mid-surface engineering strains
M	Number of axial half waves	$\gamma_{xz}^0, \gamma_{\varphi z}^0$	Transverse shear strains
N	Number of circumferential waves	$\kappa_x^0, \kappa_\varphi^0, \kappa_{x\varphi}^0$	Curvature and twist of the shell
K	Stiffness Matrix	ω_{mn}	Natural frequency, (Hz)
M	Mass Matrix		
N_0	Axial critical buckling load, (KN/m)		
f_0	Fundamental frequency, (Hz)		
β_φ, β_x	Slopes in planes x-z and φ-z		
ρ_k	Density for each layer, (kgm^{-3})		

Fig. 6 Effect of shell thickness on the optimal results for different five laminate configurations (L/R = 1, α = 0.5).

Appendix

$$L_{11} = A_{11}\frac{\partial^2}{\partial x^2} + \frac{2A_{16}}{R}\frac{\partial^2}{\partial x\partial\varphi} + \frac{A_{66}}{R^2}\frac{\partial^2}{\partial\varphi^2}$$

$$L_{12} = L_{21} = A_{16}\frac{\partial^2}{\partial x^2} + (\frac{A_{12} + A_{66}}{R})\frac{\partial^2}{\partial x\partial\varphi} + \frac{A_{26}}{R^2}\frac{\partial^2}{\partial\varphi^2}$$

$$L_{13} = -L_{31} = \frac{A_{12}}{R}\frac{\partial}{\partial x} + \frac{A_{26}}{R^2}\frac{\partial}{\partial\varphi}$$

$$L_{14} = L_{41} = B_{11}\frac{\partial^2}{\partial x^2} + (\frac{2B_{16}}{R})\frac{\partial^2}{\partial x\partial\varphi} + \frac{B_{66}}{R^2}\frac{\partial^2}{\partial\varphi^2}$$

$$L_{15} = L_{51} = B_{16}\frac{\partial^2}{\partial x^2} + (\frac{B_{12} + B_{66}}{R})\frac{\partial^2}{\partial x\partial\varphi} + \frac{B_{26}}{R^2}\frac{\partial^2}{\partial\varphi^2}$$

$$L_{22} = (A_{66} + N_a)\frac{\partial^2}{\partial x^2} + \left(\frac{2A_{26}}{R}\right)\frac{\partial^2}{\partial x\partial\varphi} + \frac{A_{22}}{R^2}\frac{\partial^2}{\partial\varphi^2} - \frac{H_{44}}{R^2}$$

$$L_{23} = -L_{32} = \frac{A_{26} + H_{45}}{R}\frac{\partial}{\partial x} + \frac{A_{22} + H_{44}}{R^2}\frac{\partial}{\partial\varphi}$$

$$L_{24} = L_{42} = B_{16}\frac{\partial^2}{\partial x^2} + \left(\frac{B_{12} + B_{66}}{R}\right)\frac{\partial^2}{\partial x\partial\varphi} + \frac{B_{26}}{R^2}\frac{\partial^2}{\partial\varphi^2} + \frac{H_{45}}{R}$$

$$L_{25} = L_{52} = B_{66}\frac{\partial^2}{\partial x^2} + \left(\frac{2B_{26}}{R}\right)\frac{\partial^2}{\partial x\partial\varphi} + \frac{B_{22}}{R^2}\frac{\partial^2}{\partial\varphi^2} + \frac{H_{44}}{R}$$

$$L_{33} = (H_{55} + N_a)\frac{\partial^2}{\partial x^2} + \left(\frac{2H_{45}}{R}\right)\frac{\partial^2}{\partial x\partial\varphi} + \frac{H_{44}}{R^2}\frac{\partial^2}{\partial\varphi^2} - \frac{A_{22}}{R^2}$$

$$L_{34} = L_{43} = \left(H_{55} - \frac{B_{12}}{R}\right)\frac{\partial}{\partial x} + \left(\frac{H_{45}}{R} - \frac{B_{26}}{R^2}\right)\frac{\partial}{\partial\varphi}$$

$$L_{35} = -L_{53} = \left(H_{45} - \frac{B_{26}}{R}\right)\frac{\partial}{\partial x} + \left(\frac{H_{44}}{R} - \frac{B_{22}}{R^2}\right)\frac{\partial}{\partial\varphi}$$

$$L_{44} = D_{11}\frac{\partial^2}{\partial x^2} + \left(\frac{2D_{16}}{R}\right)\frac{\partial^2}{\partial x\partial\varphi} + \frac{D_{66}}{R^2}\frac{\partial^2}{\partial\varphi^2} - H_{55}$$

$$L_{45} = L_{54} = D_{16}\frac{\partial^2}{\partial x^2} + \left(\frac{D_{12} + D_{66}}{R}\right)\frac{\partial^2}{\partial x\partial\varphi} + \frac{D_{26}}{R^2}\frac{\partial^2}{\partial\varphi^2} - H_{45}$$

$$L_{55} = D_{66}\frac{\partial^2}{\partial x^2} + \left(\frac{2D_{26}}{R}\right)\frac{\partial^2}{\partial x\partial\varphi} + \frac{D_{22}}{R^2}\frac{\partial^2}{\partial\varphi^2} - H_{44}$$

References

[1] Liu, T., Zhang, W., Mao, J.J. and Zheng, Y., 2019. Nonlinear breathing vibrations of eccentric rotating composite laminated circular cylindrical shell subjected to temperature, rotating speed and external excitations. *Mechanical Systems and Signal Processing*, *127*, pp.463-498.

[2] Pitton, S.F., Ricci, S. and Bisagni, C., 2019. Buckling optimization of variable stiffness cylindrical shells through artificial intelligence techniques. *Composite Structures*, *230*, p.111513.

[3] Zhang, W., Liu, T., Xi, A. and Wang, Y.N., 2018. Resonant responses and chaotic dynamics of composite laminated circular cylindrical shell with membranes. *Journal of Sound and Vibration*, *423*, pp.65-99.

[4] Matsunaga, H., 2007. Vibration and buckling of cross-ply laminated composite circular cylindrical shells according to a global higher-order theory. *International journal of mechanical sciences*, *49*(9), pp.1060-1075.

[5] Ungbhakorn, V. and Singhatanadgid, P., 2003. Similitude and physical modeling for buckling and vibration of symmetric cross-ply laminated circular cylindrical shells. *Journal of composite materials*, *37*(19), pp.1697-1712.

[6] Lam, K.Y. and Loy, C.T., 1998. Influence of boundary conditions for a thin laminated rotating cylindrical shell. *Composite structures*, *41*(3-4), pp.215-228.

[7] Lee, Y.S. and Lee, K.D., 1997. On the dynamic response of laminated circular cylindrical shells under impulse loads. *Computers & structures*, *63*(1), pp.149-157.

[8] Walker, M. and Smith, R.E., 2003. A technique for the multiobjective optimisation of laminated composite structures using genetic algorithms and finite element analysis. *Composite structures*, *62*(1), pp.123-128.

[9] Kumar, A., Chakrabarti, A. and Bhargava, P., 2013. Vibration of laminated composite cylindrical shells with cutouts using higher order theory. *CONTRIBUTORY PAPERS*, p.195.

[10] Sepiani, H.A., Rastgoo, A., Ebrahimi, F. and Arani, A.G., 2010. Vibration and buckling analysis of two-layered functionally graded cylindrical shell, considering the effects of transverse shear and rotary inertia. *Materials & Design*, *31*(3), pp.1063-1069.

[11] Wagner, H.N.R., Hühne, C., Rohwer, K., Niemann, S. and Wiedemann, M., 2017. Stimulating the realistic worst case buckling scenario of axially compressed unstiffened cylindrical composite shells. *Composite Structures*, *160*, pp.1095-1104.

[12] Mikhasev, G., Seeger, F. and Gabbert, U., 2001. Local Buckling of Composite Laminated Cylindrical Shells with Oblique Edges under External Pressure. *Technische Mechanik. Scientific Journal for Fundamentals and Applications of Engineering Mechanics*, *21*(1), pp.1-12.

[13] Geier, B., Meyer-Piening, H.R. and Zimmermann, R., 2002. On the influence of laminate stacking on buckling of composite cylindrical shells subjected to axial compression. *Composite structures*, *55*(4), pp.467-474.

[14] Labans, E., Abramovich, H. and Bisagni, C., 2019. An experimental vibration-buckling investigation on classical and variable angle tow composite shells under axial compression. *Journal of Sound and Vibration*, *449*, pp.315-329.

[15] Ng, T.Y. and Lam, K.Y., 1999. Vibration and critical speed of a rotating cylindrical shell subjected to axial loading. *Applied Acoustics*, *56*(4), pp.273-282.

[16] Liu, Y. and Chu, F., 2012. Nonlinear vibrations of rotating thin circular cylindrical

shell. *Nonlinear Dynamics*, *67*(2), pp.1467-1479.

[17]   Kassegne, S.K. and Chun, K.S., 2015. Buckling characteristic of multi-laminated composite elliptical cylindrical shells. *International Journal of Advanced Structural Engineering (IJASE)*, *7*(1), pp.1-10.

[18]   Walker, M., Reiss, T. and Adali, S., 1997. Multiobjective design of laminated cylindrical shells for maximum torsional and axial buckling loads. *Computers & structures*, *62*(2), pp.237-242.

[19]   Reddy, J.N., 2004. *Mechanics of laminated composite plates and shells: theory and analysis.* CRC press.